

ATP Acts as a Hydrotrope to Regulate the Phase Separation of NBDY Clusters

Fei Liu and Jin Wang*



Cite This: *JACS Au* 2023, 3, 2578–2585



Read Online

ACCESS |

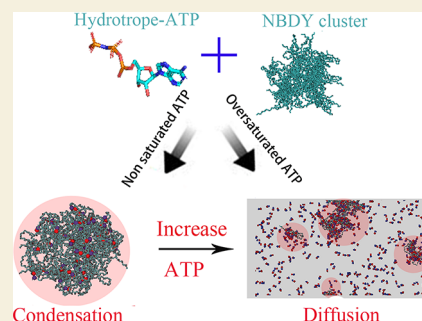
Metrics & More

Article Recommendations

Supporting Information

ABSTRACT: Nonannotated P-body dissociating polypeptide (NBDY) is a recently discovered human microprotein that has been found to be a novel component of the mRNA decapping complex. Previous studies have shown that the phosphorylation of NBDY promotes the liquid phase of the NBDY remixing in vitro. Typically, during the process of phosphorylation, a phosphate group is added to the protein through adenosine triphosphate (ATP) hydrolysis. It has been shown that ATP acts as a biological hydrotrope, affecting the phase separation of proteins in solution. In this study, we utilized simulation methods to investigate the dynamic properties of the NBDY clusters at various ATP concentrations. Our findings demonstrate that ATP can regulate the phase separation of NBDY clusters. Specifically, we identified a critical point in the concentration ratio between ATP and NBDY that exhibits a dual effect on the phase separation of NBDY. We observed that the nonsaturated ATP concentration can facilitate the formation of phase separation, while oversaturated ATP concentration promotes the diffusion of NBDY, and the oversaturated ATP-NBDY interaction impedes the phase separation of NBDY. Additionally, we found that ATPs can bind to the protein surface by aggregating into ATP clusters, which further hinders the diffusion of NBDY clusters. Our work provides general insight into the role of ATP in the phase separation of protein condensates.

KEYWORDS: Phase separation, ATP, Hydrotrope, NBDY, Molecular simulation



INTRODUCTION

Nonannotated P-body dissociating polypeptide (NBDY) is a recently discovered 7-kDa intrinsically disordered microprotein (Figure 1) that plays a critical role in the mRNA decapping complex by removing the 5' cap from mRNAs to promote 5'-to-3' decay.¹ NBDY is a component of membraneless organelles known as P-bodies, whose formation is facilitated by liquid–liquid phase separation (LLPS).^{2,3} In vitro experiments have shown NBDY can undergo LLPS in the presence of RNA, which may be a biophysical process of formation of membraneless organelles.⁴ Additionally, NBDY phosphorylation can drive liquid phase remixing in vitro.⁴ Phosphorylation-induced P-body dissociation has been observed for several P-body proteins as well.^{5,6}

Protein phosphorylation is a reversible post-translational modification that involves the addition of a phosphate group to specific amino acids, such as serine threonine, tyrosine, and histidine.⁷ The process requires the phosphate group by adenosine triphosphate (ATP) hydrolysis and is catalyzed by kinases.⁸ Recent studies have suggested that ATP, which has been described as a biological hydrotrope, can regulate the phase separation of protein condensates in solution.^{9–14} In fact, the ATP concentration in the cytoplasm can reach about 5 mM, despite only a micromole concentration being required for metabolic processes to proceed smoothly. In chemistry, ATP consists of a hydrophilic triphosphate moiety and a

hydrophobic aromatic pyrimidine base ring, making it an ideal hydrotrope.

To investigate the role of ATP in regulating the phase separation of NBDY clusters, we developed a simulation method that varied the ATP concentration. Our findings indicate that ATP can regulate the phase separation of NBDY clusters with a dual effect. These results offer valuable insights into the molecular mechanisms underlying the regulation of ATP in phase separation in protein condensates.

METHODS

Coarse-Grained Model of NBDY and ATP

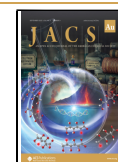
Coarse grained models have been proven successful in studying intrinsically disordered proteins (IDPs), with various models used in previous studies.^{15–21} In our study, we utilized the MOFF coarse-grained force field to model the NBDY.^{19,22} The coarse-grained model was at the amino acid residue level, and each residue of NBDY was represented by a MOFF

Received: July 20, 2023

Revised: August 16, 2023

Accepted: August 25, 2023

Published: September 4, 2023



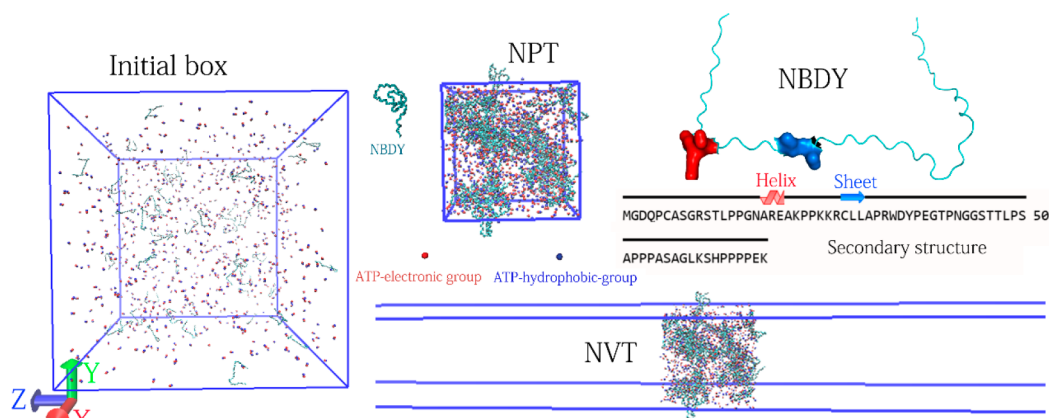


Figure 1. Initial structure of simulation and schematic diagram of slab model. The secondary structure prediction of NBDY is also presented, where black lines represent random coil, red helices represent α helix, and blue arrows represent β sheet. In the schematic diagram of the slab model, blue rectangles represent the simulation boxes, while NBDY is represented by a cyan ribbon. Each ATP is represented by an electronic bead (red) and hydrophobic bead (blue).

coarse-grained bead in our simulation model. The MOFF force field potential for proteins includes four terms:

$$U_{\text{MOFF}} = U_{\text{backbone}} + U_{\text{memory}} + U_{\text{electrostatic}} + U_{\text{contact}}$$

U_{backbone} and U_{memory} are responsible for maintaining the geometry of the protein molecules. $U_{\text{electrostatic}}$ describes electrostatic interactions between the charged residues with the Debye–Hückel theory. The last term U_{contact} is the amino-acid-type-dependent pairwise contact potential. More information on MOFF force field potential can be found in the references.^{19,22}

In our model, the ATP was represented by two coarse-grained bead based on our previous work.²³ In chemistry, ATP consists of three electronic triphosphate moieties and a hydrophobic aromatic pyrimidine base ring. Thus, one hydrophobic bead was used to represent the adenine and ribose, and one electronic bead was used to represent the three phosphate groups, each with a charge of -4 . These two beads were positioned at the center of mass of each group, respectively. The hydrophobic bead and electronic bead were connected by the harmonic spring to model ATP as a rigid liner chain.

We combined the MOFF potential of NBDY with that of ATP to describe NBDY-ATP interactions under implicit solvation. The potential between NBDY and ATP molecules includes electrostatic interaction, hydrophobic interaction, and repulsive interaction potential. The electrostatic interactions between charged residues and electronic bead of ATP were described by the Debye–Hückel theory as the $U_{\text{electrostatic}}$ term in MOFF. Hydrophobic interactions between hydrophobic residues of NBDY and hydrophobic beads of ATP were included. Only repulsive potential existed between ATP beads and nonhydrophobic and nonelectronic residues. For further details regarding the NBDY-ATP interaction potential, refer to the Supporting Information (SI).

Slab Simulation Model and Simulation Details

NBDY is a microprotein with 68 residues that lacks a defined structure due to its intrinsically disordered nature (UniProt: A0A0U1RRES). To study its behavior under different conditions of simulation, we obtained its initial structure of NBDY from the AlphaFold Protein Structure Database (<https://alphafold.ebi.ac.uk/>) and predicted its secondary

structure using computational methods (Figure 1). The results showed that NBDY is predominantly composed of random coils, with little α helix or β sheet structure (Figure 1).

To investigate the effects of the ATP concentration on NBDY clustering, we employed a slab simulation model. The strategy of slab simulation has been successfully used in previous studies to study the dynamic process of phase separation of membraneless organelles.^{16,19,22,24,25} First, we placed 50 NBDY molecules in different simulation boxes, each containing a different number of ATP molecules ranging from 50 to 2050 (Figure 1). For each box of NBDY and ATP molecules, the initial box size of NPT simulation was 100 nm \times 100 nm \times 100 nm. Then we performed NPT simulations on each system for 10^4 reduced unit time τ at reduced temperature 0.4 (the reduced unit of temperature multiplied by the Boltzmann constant k_B is used), with periodic boundary conditions and 1.0 bar pressure using Parrinello–Rahman barostat. After NPT simulation, we observed that the system underwent a packing transition, resulting in tightly packed conformation and a packed simulation box with a final size marked as $P_x \times P_y \times P_z$ (Figure 1). In most cases, P_x , P_y , and P_z were below 25 nm.

Finally, we performed NVT simulations on the packed conformations to explore the diffusion process. We increased the size of the simulation box of each system to $P_x \times P_y \times 300$ nm and a $10^6 \tau$ Langevin dynamics run in NVT ensemble on each system. The periodic boundary conditions were used in the NVT simulation. All simulations were performed with Gromacs2016²⁶ with a time τ step (1.0 unit) and $1.0 \tau^{-1}$ friction coefficient of the Langevin thermostat. To investigate the effects of temperature on the system, we performed three parallel NPT simulations on each system at temperatures of 0.4 and 0.8 (reduced units), respectively.

Data Analysis

To investigate the diffusion process of compact conformation of NBDY-ATP alone on the Z axis of the NVT simulation box, we changed the size of simulation box $P_x \times P_y \times P_z$ (where P_x , P_y , and P_z are all less than 25 nm) to $P_x \times P_y \times 300$ nm and kept the periodic boundary conditions (Figure 1). We selected the z axis of the NVT simulation box as the reaction coordinate for each frame of the trajectory and divided it into 100 windows ($i = 1-100$). To quantify the extent of phase separation, we counted the number of beads of NBDY in each

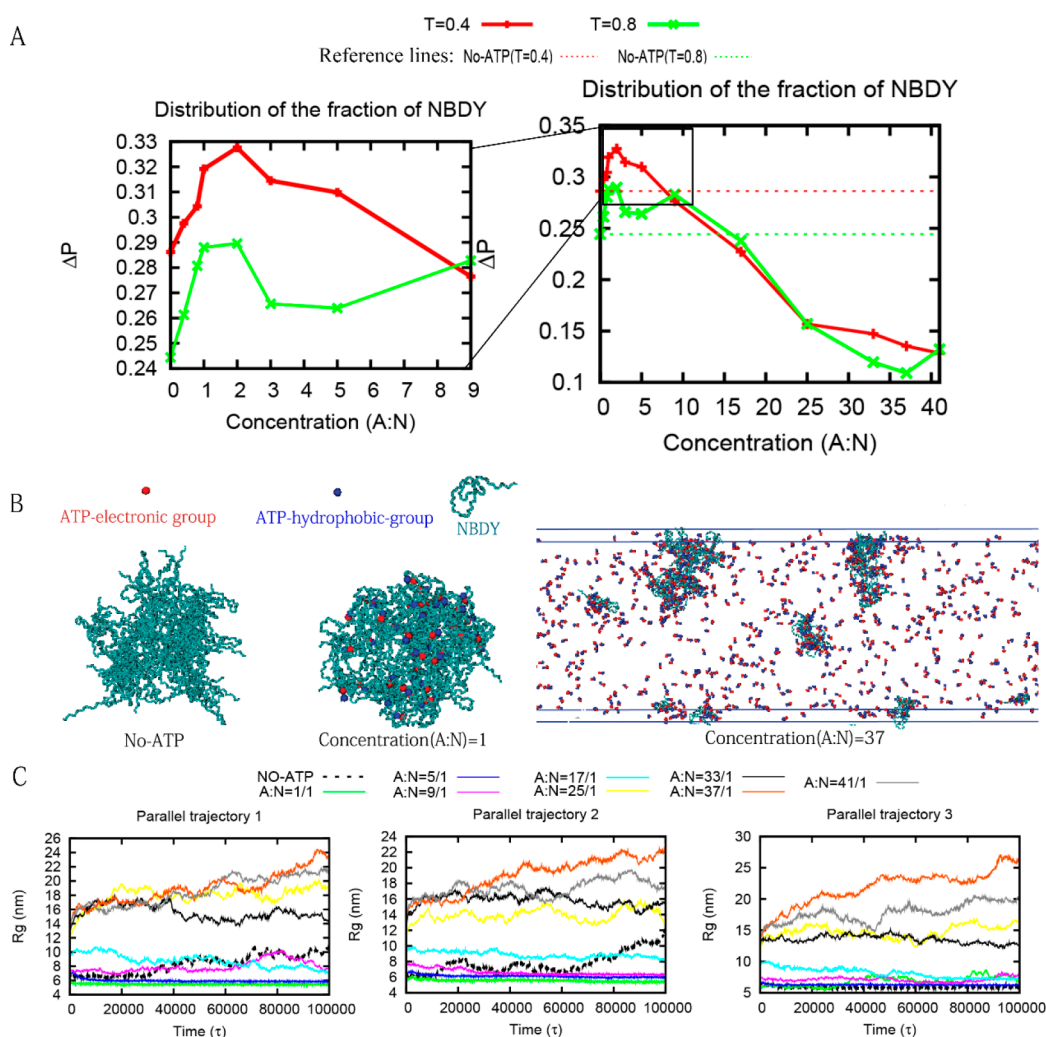


Figure 2. ATP regulates the phase separation of NBDY cluster. (A) Y-axis represents the difference of between maximum and the minimal values of the fraction of NBDY beads ΔP (see the section on [Data Analysis](#) for details). $T = 0.4$ represents the data from the simulation at reduced temperature 0.4 (the reduced unit of temperature multiplied by the Boltzmann constant k_B is used). The concentration(A:N) is the concentration ratio between ATP and NBDY, which represents the ratio between the quantities of ATP and NBDY molecules within the simulation box. The red and green dashed reference lines respectively represent the reference ΔP values of system which do not include ATP at temperatures 0.4 and 0.8, which are not coupled to the concentration(A:N). (B) Final conformation extracted from the simulation of each system. Blue rectangles represent the simulation boxes. NBDY is represented by a cyan ribbon, and each ATP is represented by an electronic bead (red) and hydrophobic bead (blue). (C) Dynamic trajectory of radius of gyration (R_g) in the unit time τ step at reduced temperature 0.4. Three parallel trajectories are shown for each system.

window, denoted as m_i , and calculated the fraction of beads $P_i = m_i/N$ ($i = 1-100$) of each window, where N is the total number of NBDY beads. We also determined the maximum and minimal values of the fraction of beads as P_{\max} and P_{\min} , respectively. A large difference between P_{\max} and P_{\min} indicates coexistence of the compactness and diffusion phases (phase separation occurs), while a smaller difference indicates a uniform system (phase separation disappears). We defined the ΔP of each system as the average value of $|P_{\max} - P_{\min}|$ along the dynamic trajectory of all three NVT parallel simulations.

Furthermore, we defined R_g by computing the radius of gyration of all of the NBDY beads in each system. We defined the number of contacts between two groups using the algorithm mindist in Gromacs with a cutoff of 0.8 nm.²⁶ Additionally, we defined RMSF by computing the average value of the root-mean-square fluctuation of atomic positions of all atoms of NBDY along the trajectory to quantify the degree of structural fluctuation.

RESULTS

ATP Regulates the Phase Separation of NBDY Clusters

We investigated the diffusion process of the compact conformation NBDY clusters across different ATP concentrations (Figure 2). Concentration(A:N) represents the ratio between the quantities of ATP and NBDY molecules within the simulation box. Our results indicate that the ATP can regulate the phase separation of NBDY. Specifically, in very low range of concentration(A:N) (<2), there is a slow monotonic increase in ΔP when concentration(A:N) increases at both temperatures of 0.4 and 0.8. As the concentration ratio between ATP and NBDY (concentration(A:N)) increases to above 10, ΔP shows a steep decreasing trend at low temperatures 0.4 and 0.8 (Figure 2A). However, it is important to note that the ΔP of the system with ATP is always higher than that of the NBDY system without ATP when then concentration(A:N) is lower than 10.

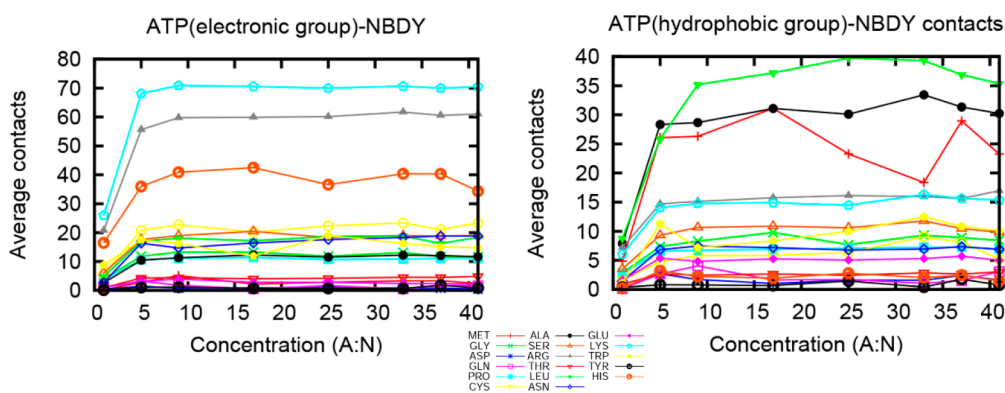


Figure 3. Y-axis represents the average number of contacts between ATP (electronic group or hydrophobic group) and 17 kinds of residue of NBDY in each frame along all three parallel dynamic trajectories. Concentration(A:N) represents the concentration ratio between ATP and NBDY.

At higher concentration(A:N) (>10), ΔP becomes smaller and lower than that of the system without ATP (Figure 2A). At lower concentration(A:N) at temperatures of 0.4 and 0.8, the system becomes more compact, resulting in a large ΔP , which indicates that ATP promotes the occurrence of the phase separation of the NBDY cluster (Figure 2A and B). Conversely, at higher concentration(A:N) at temperatures of 0.4 and 0.8, the NBDY cluster becomes less compact, with more diffusion coexisting in the system (Figure 2B). As a result, there is a smaller ΔP , which indicates that ATP disfavors the occurrence of the phase separation of the NBDY cluster (Figure 2A and B).

Furthermore, we analyzed the dynamic trajectory of R_g at a temperature of 0.4 and found that the NBDY cluster had a smaller radius of gyration when the concentration(A:N) was less than 9, and a larger radius of gyration when the concentration(A:N) was greater than 9, as compared to the system of the NBDY cluster without ATP (Figure 2C).

Oversaturated ATP-NBDY Interaction Disfavors the Phase Separation of NBDY Clusters

To understand why ATP has a dual effect on the phase separation of NBDY clusters at different concentrations (A:N), it is important to examine the interactions between molecules (Figure 3). Our analysis revealed that there are both electronic and hydrophobic interactions between ATP and most of the residues of NBDY, which peak at the point of concentration-(A:N) ≈ 10 . As concentration(A:N) exceeds 10, the number of interactions between ATP and NBDY stabilizes. In fact, concentration(A:N) ≈ 10 is the critical point for the dual effect of ATP on the phase separation of NBDY clusters. Specifically, we propose that ATP promotes the phase separation of NBDY clusters when concentration(A:N) is insufficient to maintain the saturated interaction between ATP and NBDY. Conversely, as concentration(A:N) increases and interaction between ATP and NBDY becomes oversaturated, ATP begins to hinder the phase separation of the NBDY cluster.

ATP-NBDY Interaction Affects the Interaction among NBDYs in the Clusters

We found that the oversaturated ATP-NBDY interaction may disfavor the phase separation of the NBDY cluster. Our analysis revealed that the top two numbers of electronic interaction between ATP and NBDY were ATP-LYS and ATP-ARG interactions, while the top two numbers of hydrophobic interactions between ATP and NBDY were ATP-LEU and ATP-ALA interactions (Figure 3). To investigate the detailed

mechanism of how the oversaturated ATP-NBDY interactions regulate the phase separation of the NBDY cluster, we counted the number of contacts between four key residues (LYS, ARG, LEU, and ALA) and other residues in the NBDY clusters (Figures 4, S1, and S2).

We found that, for LYS-other residue interactions in each NBDY cluster, the number of LYS-GLY, LYS-ASP, LYS-GLN, and LYS-PRO interactions decreased significantly (>20 contacts) as concentration(A:N) increased. However, the number of LYS-CYS, LYS-ALA, LYS-ARG, LYS-ASN, and LYS-LYS interactions increased below concentration(A:N) = 10 and decreased above concentration(A:N) = 10 (Figures 4A and S1). Similarly, for ARG-other residue interactions in each NBDY cluster, the number of ARG-GLY, ARG-ASP, ARG-TYR, and ARG-PRO interactions decreased significantly (>20 contacts) as concentration(A:N) increased. However, the number of ARG-ARG, ARG-LYS, and ARG-LEU interactions increased below concentration(A:N) = 10 and decreased above concentration(A:N) = 10 (Figures 4B and S1).

Moreover, for LEU-other residue interactions in each NBDY cluster, the number of LEU-ALA, LEU-TRP, and LEU-CYS interactions decreased significantly (>20 contacts) as concentration(A:N) increased. However, the number of LEU-PRO and LEU-ARG interactions increased below concentration(A:N) = 10 and decreased above concentration-(A:N) = 10 (Figures 4C and S2). For ALA-other residue interactions in each NBDY cluster, we found the number of ALA-LEU, ALA-GLY, and ALA-LEU interactions decreased significantly (>20 contacts) as concentration(A:N) increased. However, the number of ALA-PRO, ALA-CYS, ALA-LYS, and ALA-TYR interactions increased below concentration(A:N) = 10 and decreased above concentration(A:N) = 10 (Figures 4D and S2).

In summary, as concentration(A:N) increased, many electronic interactions (such as LYS-ASP and ARG-ASP), hydrophilic interactions (such as LYS-GLN and ARG-TYR), backbone chain interactions (such as LYS-GLY, ARG-GLY, and ALA-GLY), and hydrophobic interactions (such as LEU-ALA, LEU-TRP, and ALA-ALA) in each NBDY cluster were disrupted due to the increased ATP-NBDY interaction, leading to the diffusion of the compact NBDY cluster. In contrast, we found many interactions between positive charge residues and interaction between electronic and hydrophobic residues increased below concentration(A:N) = 10 and decreased above concentration(A:N) = 10, such as LYS-LYS, ARG-ARG, LYS-ARG, ARG-LEU, and LYS-ALA interactions. Nonsatu-

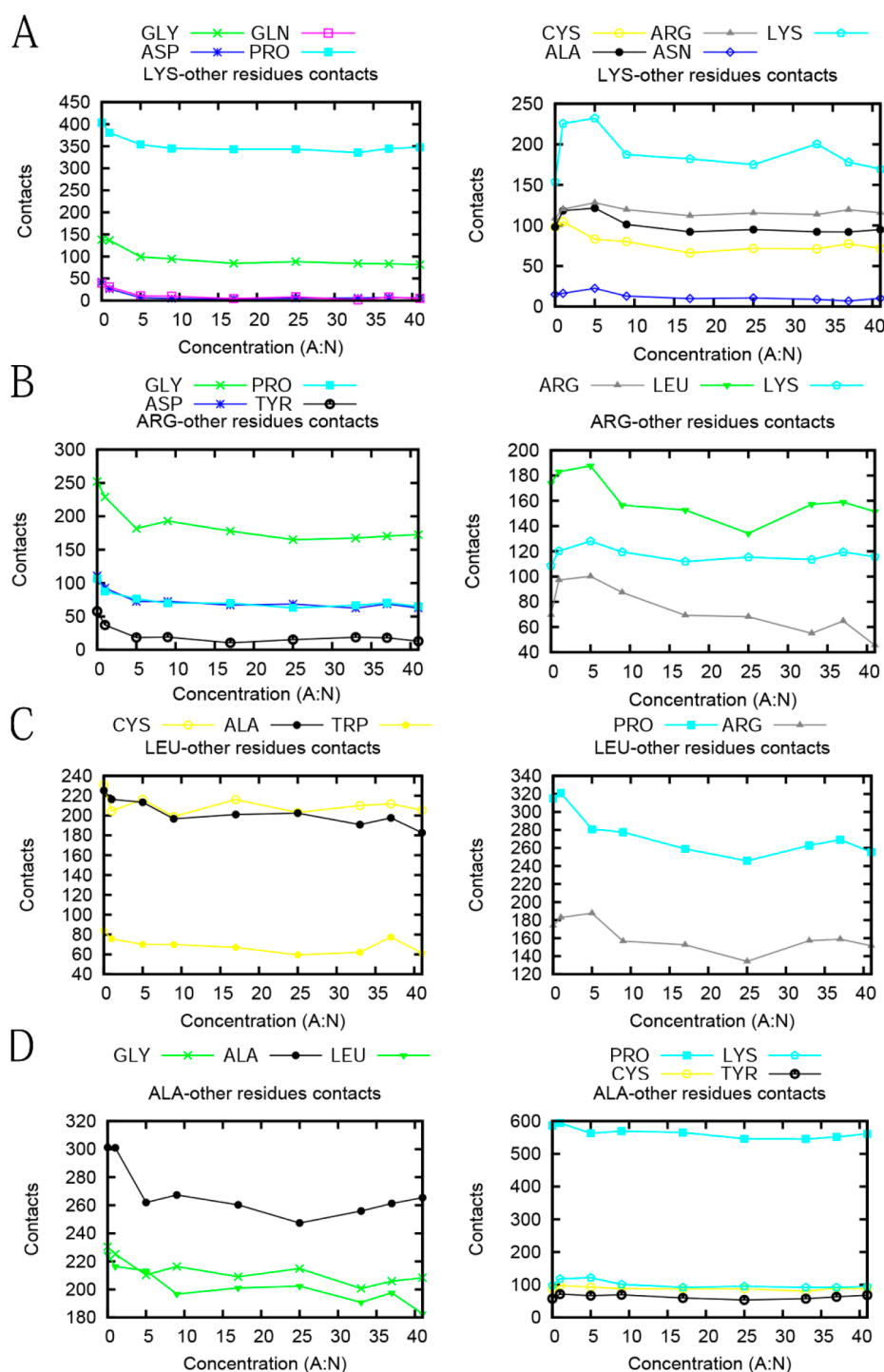


Figure 4. Y-axis represents the average number of contacts between two kinds of residues of NBDYs in each frame along all three parallel dynamic trajectories. For example, “LYS-other residues contacts” represents the number of the contact between LYS and other residues among each NBDY in cluster. Concentration(A:N) represents the concentration ratio between ATP and NBDY.

rated ATP-NBDY interactions may favor these interactions and make the cluster of NBDY more compact below concentration(A:N) = 10.

Oversaturated ATP Favors the Diffusion of NBDY

By calculating the average root-mean-square fluctuation (RMSF) of atomic positions across all atoms in NBDY over the course of the trajectory, we observed a significant increase in atomic fluctuation above concentration(A:N) = 10. Furthermore, at the concentration(A:N) exceeding 20, the

degree of fluctuation became even more drastic (Figure 5A). This suggests that the oversaturated ATP would induce more drastic diffusion of NBDY and ATP acted as a hydrotrope. Notably, we also observed a decrease in the RMSF of atomic positions from concentration(A:N) = 0 to concentration(A:N) = 5, which is consistent with the notion that ATP promotes the phase separation of the NBDY cluster when concentration(A:N) is below 10.

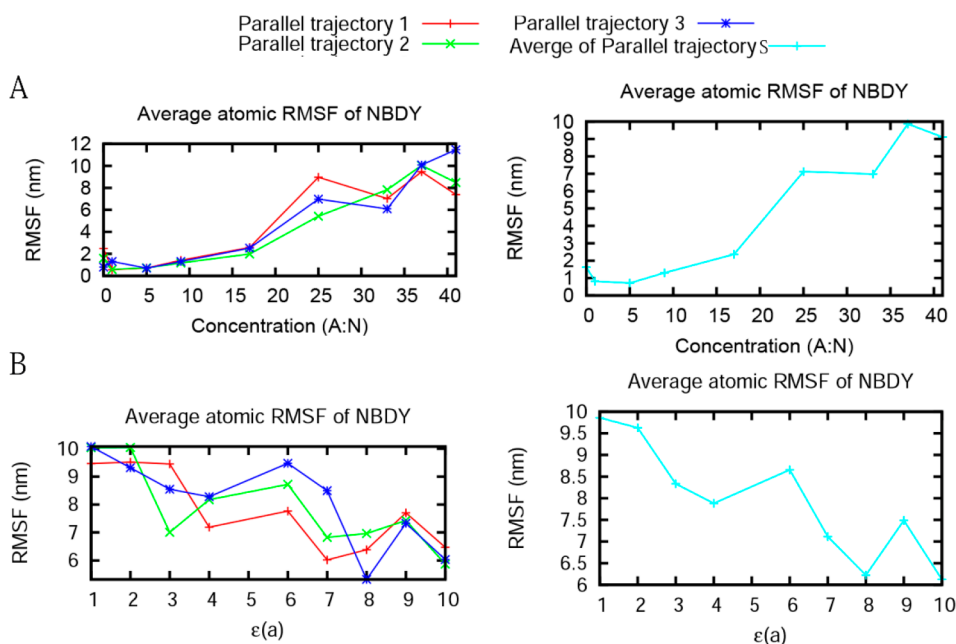


Figure 5. Average value of the root-mean-square fluctuation (RMSF) of atomic positions of all atoms of NBDY along each trajectory and average RMSF of atomic positions of all atoms of NBDY along all three parallel trajectories. (A) The X-axis represents the concentration ratio between ATP and NBDY. (B) The X-axis represents the energy parameter $\epsilon(a)$ that controls the strength of hydrophobic interaction between hydrophobic beads of ATP. A larger $\epsilon(a)$ indicates stronger hydrophobic interaction between hydrophobic beads of ATP. Concentration(A:N) of these system is 37.

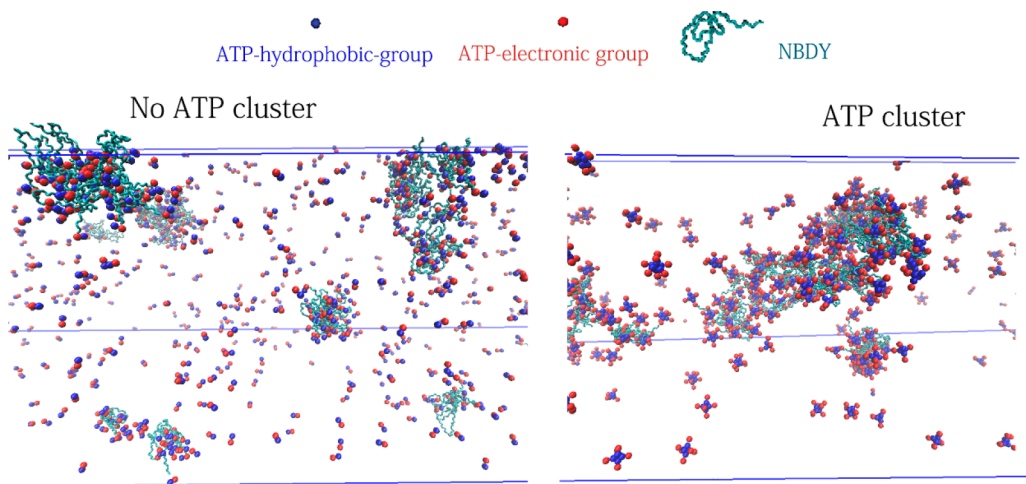


Figure 6. Final conformation extracted from the simulation of each system. Concentration(A:N) of both system is 37. For the No ATP cluster, $\epsilon(a) = 1$, while for the ATP cluster system, $\epsilon(a) = 8$.

ATP Cluster Disfavors the Diffusion of NBDY

ATP functions as a hydrotrope, which means that its hydrophobic group may assemble and form clusters in the solution. Our study investigated how the clustering of ATP affects the diffusion of NBDY clusters. We varied the energy coupling parameter $\epsilon(a)$, which governs the hydrophobic interaction strength between hydrophobic beads of ATP pertaining to the Lennard-Jones potential function, and analyzed the resulting changes in RMSF and R_g of NBDY clusters (Figures 5B and S3). Our results indicate that increasing the energy coupling parameter $\epsilon(a)$ led to a reduction in the RMSF of NBDY (Figure 5B) and the formation of ATP clusters (Figure 6). These findings suggest that ATP clustering hinders the diffusion of NBDY and promotes the phase separation of NBDY clusters (Figure 6).

DISCUSSION AND CONCLUSION

A previous study suggested that the limited number of ARG residues and oversaturated ATP-ARG interaction could lead to the breakage of TYR-ARG binding and inhibition of phase separation at high concentration of ATP.⁹ Our work supports this conclusion by demonstrating that the TYR-ARG binding is disrupted as concentration(A:N) increases. Moreover, we found that various types of interactions, such as electrostatic, hydrophilic, backbone chain, and hydrophobic interactions, are disrupted as concentration(A:N) increased. We also identified PRO and CYS as two key residues that may play a special role. The number of interactions involved in PRO or CYS fluctuates significantly at different concentration(A:N). In fact, CYS is often involved in disulfide bonds that promote protein assembly while PRO has a wide distribution in most IDPs.

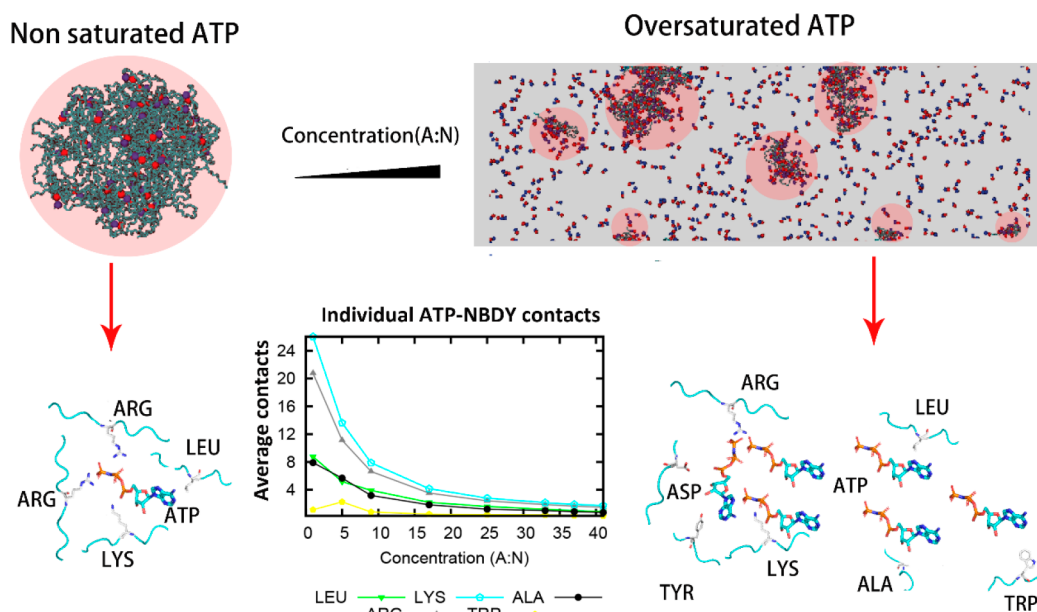


Figure 7. Final conformations (top half) extracted from the simulation of nonsaturated ATP with clear phase separation and oversaturated ATP system with the inhibition of phase separation. NBDY is represented by a cyan ribbon, and each ATP is represented by an electric charged bead (red) and hydrophobic bead (blue). In the line-stick model (bottom half), the backbone chain of NBDY is represented by a cyan line model. ATP and key residues are represented by a stick model. In the lower central region of the figure, the graph illustrates the average count of interactions between individual ATP molecules and NBDY residues at various concentration(A:N). The vertical axis depicts the mean number of hydrophobic contacts (involving LEU, ALA, and TRP) as well as electronic contacts (involving LYS and ARG) formed between individual ATP molecules and NBDY residues.

The experimental investigation has provided evidence that ATP can act as a hydrotrope to inhibit the formation of protein condensates.¹² In our work, we designed slab simulations to explore the molecular mechanism that ATP can act as a hydrotrope of NBDY condensates. We discovered a critical point of concentration(A:N) exists for the dual effect of ATP on the phase separation of NBDY. Our study demonstrated that the LYS-LYS, ARG-ARG, LYS-ARG, ARG-LEU, and LYS-ALA interactions made the cluster of NBDY more compact when below concentration(A:N) = 10. Normally, the interactions between the homogeneous charge residues and the interactions between the charge residues and hydrophobic residues are hard to form. However, we believe that ATP plays a special role in the formation of these interactions. ATP has -4 charge and hydrophobic group; it can simultaneously bind to more than one positive charge residue and the hydrophobic residue when its concentration is nonsaturated. ATP can act as mediator between these residues (Figure 7). In other words, ATP can act as the junction between different NBDYs and make the cluster of NBDYs more compact, which facilitates the formation of a phase separation (Figure 7). When ATP is oversaturated, each residue of NBDY can be surrounded by more than one ATP, which leads to the breakdown of the interactions between NBDYs and the inhibition of phase separation (Figure 7).

Analyzed data present support for the proposed mechanisms, as illustrated in Figure 7, detailing the average number of contacts between individual ATP molecules and NBDY residues. Notably, in instances of nonsaturated ATP concentration, individual ATP establishes numerous contacts with NBDY residues, implying its role as a pivotal bridge connecting distinct NBDY units. Conversely, when the ATP concentration reaches oversaturation, the average contact count between individual ATP molecules and NBDY residues

diminishes significantly. This reduction follows a trend toward approaching zero with increasing ATP concentration (Figure 7), suggesting the potential for multiple ATP molecules to collectively share a single contact point with each NBDY residue.

Furthermore, corroborating both empirical experimentation and theoretical insights, ATP's established multivalence emerges as a key driver in inducing condensate formation through phase separation.^{9,11,13} These investigations provide direct evidence substantiating our proposed model, wherein ATP acts as a junction between diverse NBDY entities, enhancing the compactness of the NBDY clusters. Notably, existing research^{9,12–14} underscores ATP's capability in disrupting protein–protein and protein–RNA interactions, further reinforcing our model's premise that ATP contributes to dismantling interactions between NBDYs, consequently inhibiting phase separation.

Previous evidence has shown that ATPs can bind to the protein surface by aggregating into ATP clusters.¹¹ Our studies clearly indicate that the ATP cluster disfavors the diffusion of NBDY and favors the phase separation of the NBDY cluster. This observation may provide general insight into the role of ATP in the phase separation of certain protein condensates.

■ ASSOCIATED CONTENT

SI Supporting Information

The Supporting Information is available free of charge at <https://pubs.acs.org/doi/10.1021/jacsau.3c00391>.

Methods of the Hamiltonian of NBDY-ATP interaction and supplementary Figures S1–S3 (PDF)

AUTHOR INFORMATION

Corresponding Author

Jin Wang – Wenzhou Institute, University of Chinese Academy of Sciences, Wenzhou, Zhejiang 325001, China; Department of Chemistry and Physics, State University of New York at Stony Brook, Stony Brook, New York 11794, United States; orcid.org/0000-0002-2841-4913; Email: jin.wang.1@stonybrook.edu

Author

Fei Liu – Wenzhou Institute, University of Chinese Academy of Sciences, Wenzhou, Zhejiang 325001, China; orcid.org/0009-0005-1400-9051

Complete contact information is available at:
<https://pubs.acs.org/10.1021/jacsau.3c00391>

Author Contributions

CRedit: **Fei Liu** conceptualization, data curation, formal analysis, funding acquisition, investigation, methodology, project administration, resources, software, supervision, validation, visualization, writing-original draft, writing-review & editing; **Jin Wang** conceptualization, data curation, formal analysis, investigation, methodology, project administration, resources, software, supervision, validation, visualization, writing-original draft, writing-review & editing.

Notes

The authors declare no competing financial interest.

ACKNOWLEDGMENTS

Fei Liu acknowledges support from Natural Science Foundation of China (grant numbers 22103040). We thank Prof. Chun Tang for bringing our attention to the experimental studies of phase separation under the various ATP concentrations and helpful discussions.

REFERENCES

- (1) D'Lima, N. G.; Ma, J.; Winkler, L.; Chu, Q.; Loh, K. H.; Corpuz, E. O.; Budnik, B. A.; Lykke-Andersen, J.; Saghatelian, A.; Slavoff, S. A. A human microprotein that interacts with the mRNA decapping complex. *Nat. Chem. Biol.* **2017**, *13* (2), 174–180.
- (2) Maccaroni, K.; La Torre, M.; Burla, R.; Saggio, I. Phase Separation in the Nucleus and at the Nuclear Periphery during Post-Mitotic Nuclear Envelope Reformation. *Cells* **2022**, *11* (11), 1749.
- (3) Shin, Y. Rich Phase Separation Behavior of Biomolecules. *Mol. Cells* **2022**, *45* (1), 6–15.
- (4) Na, Z.; Luo, Y.; Cui, D. S.; Khitun, A.; Smelyansky, S.; Loria, J. P.; Slavoff, S. A. Phosphorylation of a Human Microprotein Promotes Dissociation of Biomolecular Condensates. *J. Am. Chem. Soc.* **2021**, *143* (32), 12675–12687.
- (5) Aizer, A.; Kafri, P.; Kalo, A.; Shav-Tal, Y. The P body protein Dcp1a is hyper-phosphorylated during mitosis. *PLoS One* **2013**, *8* (1), No. e49783.
- (6) Bearss, J. J.; Padi, S. K.; Singh, N.; Cardo-Vila, M.; Song, J. H.; Mouneimne, G.; Fernandes, N.; Li, Y.; Harter, M. R.; Gard, J. M.; Cress, A. E.; Peti, W.; Nelson, A. D.; Buchan, J. R.; Kraft, A. S.; Okumura, K. EDC3 phosphorylation regulates growth and invasion through controlling P-body formation and dynamics. *EMBO Rep* **2021**, *22* (4), No. e50835.
- (7) Potel, C. M.; Lin, M. H.; Heck, A. J. R.; Lemeer, S. Widespread bacterial protein histidine phosphorylation revealed by mass spectrometry-based proteomics. *Nat. Methods* **2018**, *15* (3), 187–190.
- (8) Kresge, N.; Simoni, R. D.; Hill, R. L. The process of reversible phosphorylation: the work of Edmond H. Fischer. *J. Biol. Chem.* **2011**, *286* (3), No. e1.
- (9) Ren, C. L.; Shan, Y.; Zhang, P.; Ding, H. M.; Ma, Y. Q. Uncovering the molecular mechanism for dual effect of ATP on phase separation in FUS solution. *Sci. Adv.* **2022**, *8* (37), No. eabo7885.
- (10) Sarkar, S.; Mondal, J. Mechanistic Insights on ATP's Role as a Hydrotrope. *J. Phys. Chem. B* **2021**, *125* (28), 7717–7731.
- (11) Hu, G.; Ou, X.; Li, J. Mechanistic Insight on General Protein-Binding Ability of ATP and the Impacts of Arginine Residues. *J. Phys. Chem. B* **2022**, *126* (25), 4647–4658.
- (12) Patel, A.; Malinowska, L.; Saha, S.; Wang, J.; Alberti, S.; Krishnan, Y.; Hyman, A. A. ATP as a biological hydrotrope. *Science* **2017**, *356* (6339), 753–756.
- (13) Sridharan, S.; Kurzawa, N.; Werner, T.; Gunthner, I.; Helm, D.; Huber, W.; Bantscheff, M.; Savitski, M. M. Proteome-wide solubility and thermal stability profiling reveals distinct regulatory roles for ATP. *Nat. Commun.* **2019**, *10* (1), 1155.
- (14) Aida, H.; Shigeta, Y.; Harada, R. The role of ATP in solubilizing RNA-binding protein fused in sarcoma. *Proteins* **2022**, *90* (8), 1606–1612.
- (15) Benayad, Z.; von Bulow, S.; Stelzl, L. S.; Hummer, G. Simulation of FUS Protein Condensates with an Adapted Coarse-Grained Model. *J. Chem. Theory Comput* **2021**, *17* (1), 525–537.
- (16) Dignon, G. L.; Zheng, W.; Kim, Y. C.; Best, R. B.; Mittal, J. Sequence determinants of protein phase behavior from a coarse-grained model. *PLoS Comput. Biol.* **2018**, *14* (1), No. e1005941.
- (17) Regy, R. M.; Thompson, J.; Kim, Y. C.; Mittal, J. Improved coarse-grained model for studying sequence dependent phase separation of disordered proteins. *Protein Sci.* **2021**, *30* (7), 1371–1379.
- (18) Dannenhoffer-Lafage, T.; Best, R. B. A Data-Driven Hydrophobicity Scale for Predicting Liquid-Liquid Phase Separation of Proteins. *J. Phys. Chem. B* **2021**, *125* (16), 4046–4056.
- (19) Latham, A. P.; Zhang, B. Maximum Entropy Optimized Force Field for Intrinsically Disordered Proteins. *J. Chem. Theory Comput* **2020**, *16* (1), 773–781.
- (20) Tessei, G.; Schulze, T. K.; Crehuet, R.; Lindorff-Larsen, K. Accurate model of liquid-liquid phase behavior of intrinsically disordered proteins from optimization of single-chain properties. *Proc. Natl. Acad. Sci. U. S. A.* **2021**, *118* (44), No. e2111696118.
- (21) Latham, A. P.; Zhang, B. Improving Coarse-Grained Protein Force Fields with Small-Angle X-ray Scattering Data. *J. Phys. Chem. B* **2019**, *123* (5), 1026–1034.
- (22) Latham, A. P.; Zhang, B. On the stability and layered organization of protein-DNA condensates. *Biophys. J.* **2022**, *121* (9), 1727–1737.
- (23) Liu, F.; Ji, Q.; Wang, H.; Wang, J. Mechanochemical Model of the Power Stroke of the Single-Headed Motor Protein KIF1A. *J. Phys. Chem. B* **2018**, *122* (49), 11002–11013.
- (24) Dignon, G. L.; Zheng, W.; Best, R. B.; Kim, Y. C.; Mittal, J. Relation between single-molecule properties and phase behavior of intrinsically disordered proteins. *Proc. Natl. Acad. Sci. U. S. A.* **2018**, *115* (40), 9929–9934.
- (25) Chu, W. T.; Wang, J. Thermodynamic and sequential characteristics of phase separation and droplet formation for an intrinsically disordered region/protein ensemble. *PLoS Comput. Biol.* **2021**, *17* (3), No. e1008672.
- (26) Hess, B.; Kutzner, C.; van der Spoel, D.; Lindahl, E. GROMACS 4: Algorithms for Highly Efficient, Load-Balanced, and Scalable Molecular Simulation. *J. Chem. Theory Comput* **2008**, *4* (3), 435–47.